

Spinodal decomposition in binary mixtures

Roberto Mauri,^{1,2} Reuel Shinnar,¹ and George Triantafyllou²

¹*Department of Chemical Engineering, City College of CUNY, New York, New York 10031*

²*The Benjamin Levich Institute, City College of CUNY, New York, New York 10031*

(Received 11 October 1994; revised manuscript received 19 May 1995)

We study the early stage of the phase separation of a binary mixture far from its critical point of demixing. Whenever the mixture of two mutually repulsive species is quenched to a temperature below its critical point of miscibility, the effect of the enthalpic repulsive force prevails upon the entropic tendency to mix, so that the system eventually separates into two coexisting phases. We have developed a highly nonlinear model, in close analogy with the linear theory of Cahn and Hilliard, where a generalized free energy is defined in terms of two parameters ψ and a , the first describing the equilibrium composition of the two phases, and the second denoting a characteristic length scale that is inversely proportional to the equilibrium surface tension. The linear stability analysis predicts that any perturbation of the initial mixture composition with wave number k smaller than $\sqrt{2\psi}/a$ will grow exponentially in time, with a maximum growth corresponding to $k_{\max} = \sqrt{\psi}/a$. A numerical solution of the equation shows that nonlinear effects saturate the exponential growth, and that the concentration distribution tends to a steady state, periodic profile with wavelength $\lambda = 2\pi a/\sqrt{\psi}$ corresponding to the fastest growing mode of the linear regime. The main result of our theoretical model is that this steady state does not depend on the form of the initial perturbation to the homogeneous composition profile.

PACS number(s): 64.70.Ja, 64.60.Cn, 64.60.Ht, 64.75.+g

I. INTRODUCTION

In this work we present a theoretical model of the early stage of phase separation, in the case where the mixture is quenched into the unstable region of the miscibility gap. This process, called spinodal decomposition [1], is a particular case of first-order phase transitions. It is characterized by the fact that concentration fluctuations grow instead of decaying, and therefore it requires no activation energy, in contrast to nucleation, which occurs in the metastable region of the miscibility gap.

First-order phase transitions were first observed in alloys, glasses, and polymer solutions [2], and only more recently have experiments been conducted on simple liquids and binary liquid mixtures. In a pioneering series of articles by Goldberg and co-workers [3] and Wong and Knobler [4], it was shown that phase separation takes place in two stages: in the first stage long-wavelength, delocalized concentration fluctuations grow exponentially, until they coagulate into metastable drops; then, in the late stage of separation, the characteristic droplet radius R grows in time like $R \propto t^m$, where $m = \frac{1}{3}$ in the early, purely diffusive stage [5], and $m = 1$ at a later time, where surface tension effects become dominant [6]. More recently, by using a density-matched system to suppress gravity effects, these measurements were repeated and improved [7], by using both light-scattering and direct visualization techniques.

In this work we study the first stage of phase separation, i.e., spinodal decomposition, assuming that a binary mixture is quenched well below its coexistence curve. Therefore, unlike most of the previous treatments, our system is far from its critical point and therefore non-

linear terms cannot be neglected, except for very short times. At the basis of our theoretical approach is the thermodynamic theory proposed by Cahn and Hilliard [8], where all interactions are assumed to be incorporated into the free energy of formation, with no further effects needing to be considered. This approach was generalized and justified microscopically by Langer [9], Binder [10], and Kawasaki and Ohta [11], showing that it is valid provided that all time and length scales are large enough that all fluctuations have died out and the only "slow" variables are the molar fractions of the two species composing the mixture. Now, the linearized form of this theory [8, 12] seems to describe well the early-time dynamics of spinodal decomposition, and in fact it has been extended to describe polymer blends by deGennes [13], Pincus [14], and Binder [15]. However, as at later times the local composition of the mixture moves away from its mean value, the linear approximation is not valid any more [15, 16], and nonlinear effects become dominant. One of the main contributions of this work is to recognize the importance of nonlinear effects and show that, once they are considered, a system subjected to an initial small perturbation in composition tends to assume a stationary, periodic composition profile, independent of the form of the initial perturbation. This corresponds to the formation of small drops in a metastable state, which later will grow due to diffusion and coalescence [4, 5].

This paper is organized as follows. In Sec. II we present the basic thermodynamic theory, showing that the nonlinear terms arise naturally from it. Then, in Sec. III, a continuity equation for the local composition is derived and solved analytically, for short times, and numerically, for longer times, showing that the con-

centration distribution tends to a steady-state periodic profile.

II. STATIONARY STATE

A. Classical thermodynamics

We consider a homogeneous mixture of two species A and B with molar fractions x_A and x_B , respectively, contained in a closed system at temperature T and pressure P . The equilibrium state of this system is such that it minimizes the molar Gibbs energy of mixing, Δg , subjected to the constraint that the total number of moles is conserved. Here

$$\Delta g = g - (g_A x_A + g_B x_B), \quad (1)$$

where g is the energy of the mixture, while g_A and g_B are the molar free energies of pure species A and B , respectively, at temperature T and pressure P . Δg is the sum of an ideal part Δg^{id} and a so-called excess part g^{ex} , with

$$\Delta g^{\text{id}} = RT[x_A \ln x_A + x_B \ln x_B], \quad (2)$$

where R is the gas constant, while the excess molar free energy is typically expressed through the Margules correlation [17]

$$g^{\text{ex}} = RTx_A x_B [\Psi_A x_A + \Psi_B x_B], \quad (3)$$

where Ψ_A and Ψ_B are experimentally determined functions of T and P . In the following, we shall assume that P is fixed, so that the physical state of the mixture depends only on T and x_A . Also, for the sake of simplicity, in the first part of our work we shall assume that species A and B have physical properties that are close enough to have

$$\Psi_A = \Psi_B = \Psi, \quad (4)$$

so that the excess molar free energy (3) reduces to the Flory-Huggins expression [18]

$$g^{\text{ex}} = RT\Psi x_A x_B. \quad (5)$$

It should be noted that expression (3) for the free energy refers to equilibrium states; yet, in this work we apply it to states far from equilibrium. In Appendix A we show that this can be done for gas mixtures, showing that Ψ is proportional to the second virial coefficient and characterizes the tendency of equal molecules to aggregate. For liquid mixtures, although the analysis of Appendix A is not applicable, the equilibrium expression for the free energy is still valid, provided that the condition of local equilibrium is satisfied. That means that the mean square amplitude of the fluctuations in composition is smaller than the square of the composition itself, a condition that is generally referred to as the Ginzburg criterion [19].

The interesting point for first-order phase transitions is that below a certain critical temperature T_c the molar free energy given by (2) and (3) [or (5)] is a double-well

potential, as shown in Fig. 1(a). Now it is well known that the molar free energy can be written as [17]

$$g/RT = \mu_A x_A + \mu_B x_B, \quad (6)$$

where μ_A and μ_B denote the chemical potential of species A and B in solution, respectively, i.e.,

$$\mu_A = \frac{1}{RT} \frac{\partial (ng)}{\partial n_A}, \quad \mu_B = \frac{1}{RT} \frac{\partial (ng)}{\partial n_B}. \quad (7)$$

Here n_A and n_B denote the number of moles of species A and B , respectively, and $n = n_A + n_B$. Differentiating Eq. (6) and applying the Gibbs-Duhem relation, after easy manipulations, we obtain

$$\mu_A = \frac{g}{RT} + \frac{x_B}{RT} \frac{dg}{dx_A}, \quad \mu_B = \frac{g}{RT} + \frac{x_A}{RT} \frac{dg}{dx_B}, \quad (8)$$

where the derivatives are taken at constants T and P . From here we see that the two quantities $\phi = x_A$ and

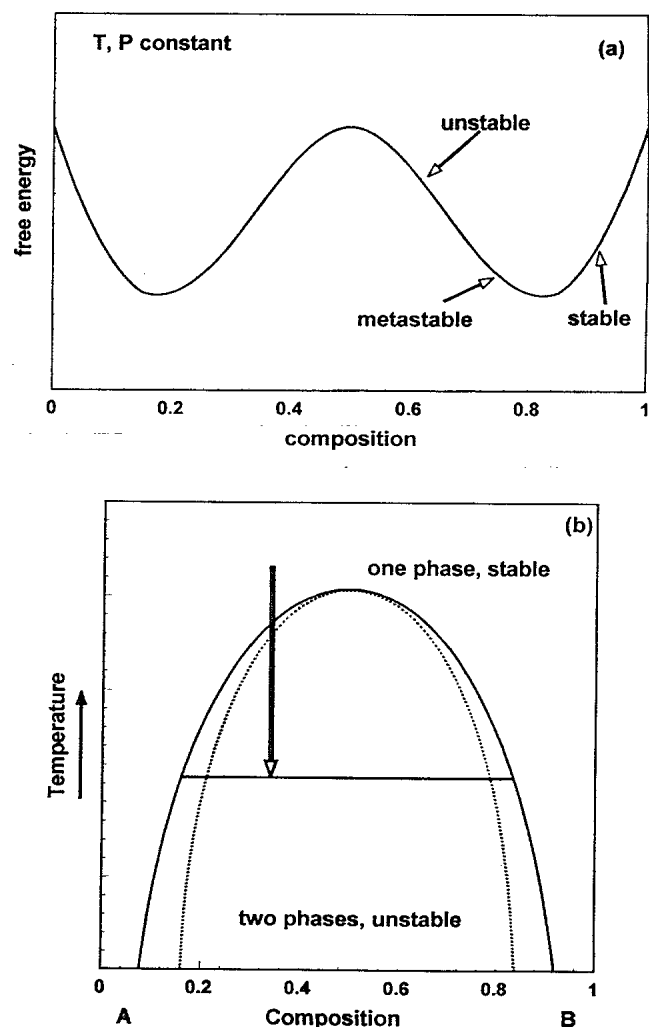


FIG. 1. (a) Gibbs free energy of binary mixtures as a function of composition. (b) Coexistence (continuous line) and spinodal (dashed line) curves.

$\mu = \mu_A - \mu_B$ are thermodynamically conjugated, that is

$$\mu = \frac{d(g/RT)}{d\phi}. \quad (9)$$

From its definition, the chemical potential μ is given by the following expression:

$$\mu = \mu_0 + \ln \frac{\phi}{1-\phi} + \Psi(1-2\phi), \quad (10)$$

with $\mu_0 = (g_B - g_A)/RT$.

Now, imposing that the stability condition $\partial^2 g/\partial\phi^2 \geq 0$ is satisfied, we find

$$|\phi - \frac{1}{2}| \leq |\phi_s - \frac{1}{2}| = \frac{1}{2} \left(\frac{\Psi - 2}{\Psi} \right)^{1/2}, \quad (11)$$

which defines the so-called spinodal curve $\phi_s(T)$, and depends on the function $\Psi = \Psi(T)$, that we assume to know. Consistent with assumption (4), the spinodal curve is symmetric about $\phi_c = \frac{1}{2}$, which corresponds to the value $\Psi_c = 2$ [cf. Eq. (11)] at the critical point. Here we have three coexisting phases and two components, so that the critical temperature T_c is determined uniquely for any given pressure. These values of ϕ_c and T_c characterize the critical point, where the onset of instability occurs: when $\phi = \phi_c$, for $T > T_c$ (i.e., $\Psi < 2$) the system is entirely miscible, while for $T < T_c$ (i.e., $\Psi > 2$) the mixture will separate into two distinct phases. The compositions ϕ_e of these two phases at equilibrium are such to minimize Δg in (1)-(3), so that by imposing $\mu = \partial g/\partial\phi = \mu_0$, in Eq. (10), we obtain the well-known mean field self-consistency equation [19]

$$(\phi_e - \frac{1}{2}) = \frac{1}{2} \tanh[\Psi(\phi_e - \frac{1}{2})], \quad (12)$$

which near the critical point can be approximated as

$$|\phi_e - \frac{1}{2}| = \frac{\sqrt{3}}{2} \left(\frac{\Psi - 2}{2} \right)^{1/2}. \quad (13)$$

This is the implicit analytic expression of the coexistence curve $\phi_e(T)$ which, in agreement with its physical interpretation, satisfies the following inequality:

$$|\phi_s - \frac{1}{2}| \leq |\phi_e - \frac{1}{2}|, \quad (14)$$

showing that the coexistence curve is always external to the spinodal curve [see Fig. 1(b)]. Note that, when $\Psi \gg 1$, both spinodal and coexistence curves reduce to $\phi = 0$ and $\phi = 1$.

B. Generalized potential

Until now, all effects of spatial inhomogeneity have not been taken into account in our thermodynamic formulation. Following Cahn and Hilliard [8], we consider the total generalized free energy G as the following volume average:

$$G = \bar{g} = \frac{1}{V} \int \tilde{g} \, d\mathbf{r}, \quad (15)$$

where \tilde{g} is the generalized specific free energy, which in

turn depends both on the concentration and on its space derivatives. The function \tilde{g} then is expanded in a Taylor series about the homogeneous concentration, so that, considering the isotropy of the medium and neglecting fourth-order gradient terms, we obtain

$$\tilde{g}(\phi, \nabla\phi, \nabla\nabla\phi, \dots) = g(\phi) + C_1(\nabla\phi)^2 + C_2\nabla^2\phi + \dots, \quad (16)$$

where C_1 and C_2 are temperature-dependent coefficients, and we have considered that $\tilde{g}(\phi, 0, 0, \dots) = g(\phi)$. Here and in the following we assume that the molar volumes of the two species are equal to each other, so that gravity effects can be ignored. Therefore, apart from a constant factor, molar and volume specific free energies are equal to each other.

Now, the integral in Eq. (15) is evaluated, subjected to no-flux or periodic boundary conditions on the boundary of the volume V , and to the additional constraint that the total mass be conserved, i.e.,

$$\bar{\phi} = \phi_0. \quad (17)$$

Therefore, due to the above-mentioned boundary conditions, the contribution of the last term in Eq. (16) to the generalized free energy is zero, and we obtain

$$G = \frac{1}{V} \int [g(\phi) + \frac{1}{2}RTa^2(\nabla\phi)^2] d\mathbf{r}, \quad (18)$$

where we have assumed that $C_1 = 1/2RTa^2$ is positive, since it takes energy to form spatial inhomogeneity, with a representing the typical length of spatial inhomogeneities in composition. As shown by van der Waals [20], a is inversely proportional to the surface tension between the two phases, and, as such, is a small length, typically $\approx 0.1 \mu\text{m}$. Equation (18) is generally referred to as the Landau-Ginzburg extension of the Ornstein-Zernike free energy form [19]. Again, it should be stressed that this expression contains only the leading-order term in expansion (16), and therefore it is valid only when the concentration gradient is not too large. This condition is equivalent to the Ginzburg criterion [16, 19] stating that the mean square amplitude of the changes in composition is smaller than the square of the mean composition, i.e.,

$$\overline{(\phi - \phi_0)^2} \ll \phi_0^2. \quad (19)$$

Now, at equilibrium, the generalized free energy is minimized. Therefore, applying the Euler-Lagrange equation to (18), subjected to the composition conservation constraint (17) and periodic or no-flux boundary conditions, we obtain [8]

$$\bar{\mu}(\phi) = \frac{1}{RT} \frac{\delta\tilde{g}(\phi)}{\delta\phi(\mathbf{r})} = \mu(\phi) - a^2\nabla^2\phi = \gamma, \quad (20)$$

which defines the generalized chemical potential $\bar{\mu}$, where γ is a Lagrangian multiplier introduced by the subsidiary condition (17) and depends on ϕ_0 . In particular, $\gamma = 0$ when $\phi_0 = \frac{1}{2}$, due to symmetry. In this case, near the critical point and defining $\phi = \frac{1}{2}(1 + u)$, Eq. (20) in one dimension reads

$$u_{zz} + 2\psi u - \frac{4}{3}u^3 = 0, \quad (21)$$

with $u_z = du/dz$, and $\psi = \Psi - 2$, where $O(u^5)$ terms have been neglected and the z coordinate has been scaled in terms of a . This equation can be solved exactly, imposing that u tends to its equilibrium values, $u_e = \sqrt{3\psi/2}$ at infinity and that the interface is located at $z = 0$, that is $u(0) = 0$ and $u(\infty) = u_e$, finding [21]

$$u(z) = u_e \tanh[\sqrt{\psi}z]. \quad (22)$$

Now, this solution, although it corresponds to an absolute minimum of the free energy, is in no way unique, as the general solution of Eq. (21) is a family of periodic functions, corresponding to relative minima of the free energy (see Novick-Cohen and Segel [22]). In fact, imposing that $u(0) = 0$ and $u_z(0) = \sqrt{\frac{3}{2}}\psi\alpha$, with $\alpha \leq 1$, we find

$$u(\bar{z}) = \beta u_e \operatorname{sn}_k \left(\frac{\alpha}{\beta} \sqrt{\psi}z \right), \quad (23)$$

where $\beta = \sqrt{1 - \sqrt{1 - \alpha^2}}$, and sn_k is Jacobi's elliptic function with parameter $k = \sqrt{2(\beta/\alpha)^2 - 1}$. The Jacobi elliptic function is defined as $\operatorname{sn}_k(x) = \sin \phi$, where $\phi = \operatorname{am}_k(x)$ is the amplitude of the incomplete elliptic integral of the first kind $F(k, \phi)$. This solution shows that $|u(z)|$ is always smaller than u_e for any z , and is equal to u_e only when $z \rightarrow \infty$ and $\alpha = 1$, that is, when the concentration profile is given by Eq. (22). In the other limit case, when $\alpha \ll 1$, Eq. (23) reduces to the trivial sinusoidal profile

$$u(z) = \frac{\alpha}{\sqrt{2}} u_e \sin \sqrt{2\psi}z, \quad (24)$$

with a period λ_{\min} which, in dimensional form, equals $\pi a \sqrt{2/\psi}$. In general, for $0 < \alpha < 1$, the periodic solution (23) has a period

$$\lambda = a \frac{4\beta}{\alpha\sqrt{\phi}} \int_0^{\pi/2} \frac{d\theta}{\sqrt{1 - k^2 \sin^2 \theta}}, \quad (25)$$

where k is Jacobi's parameter. As expected, $\lambda \rightarrow \infty$ as $\alpha \rightarrow 1$, while $\lambda \rightarrow \lambda_{\min}$ as $\alpha \rightarrow 0$. Therefore, the general solution of (21) is a family of periodic functions, with periods λ ranging from $\pi a \sqrt{2/\psi}$ to infinity. Now, among all these stationary solutions, only one represents the stable, steady-state composition profile that the system will adopt after long time, as will be explained in Sec. III B. This stationary solution in general corresponds to a metastable state, with $|u| < u_e$, where, in the absence of any destabilizing mechanism, the system will remain indefinitely.

III. EQUATION OF MOTION AND DYNAMICAL THEORY

According to the phenomenological relations of irreversible thermodynamics, the mass flow rates \mathbf{J}_A and \mathbf{J}_B of species A and B , respectively, are linearly related to the gradients of their chemical potentials through diffusivity coefficients [23]. Then after easy manipulations [22], defining the net flux $\mathbf{J} = \mathbf{J}_A - \mathbf{J}_B$ we find the following constitutive relation:

$$\mathbf{J} = -D\nabla\bar{\mu}, \quad (26)$$

where $D = D(\phi)$ is an effective composition-dependent diffusion coefficient, while $\bar{\mu}$ is given by [see Eq. (20)]

$$\bar{\mu} = \mu_0 + \log \frac{\phi}{1-\phi} + \Psi_+(1-2\phi) - \Psi_-(1-6\phi+6\phi^2) - a^2\nabla^2\phi, \quad (27)$$

where $\Psi_+ = (\Psi_A + \Psi_B)/2$ and $\Psi_- = (\Psi_A - \Psi_B)/2$. Now the constitutive equation (26) for the mass flux can be substituted into the usual continuity equation in terms of the concentration $\phi(\mathbf{r}, t)$ at location \mathbf{r} and time t of species A ,

$$\frac{\partial\phi}{\partial t} + \nabla \cdot \mathbf{J} = 0. \quad (28)$$

This dynamical equation is consistent with the previous expressions (18) and (20) for the generalized specific free energy and chemical potential. In fact, considering that the specific energy dissipated per unit time equals the product of the mass flux by the gradient of the chemical potential [23], i.e.,

$$E = -RT\mathbf{J} \cdot \nabla\bar{\mu}, \quad (29)$$

it is easy to see that mean energy dissipation equals the time derivative of the mean free energy,

$$\frac{d}{dt}\bar{g} = -\bar{E}, \quad (30)$$

where no-flux or periodic boundary conditions have been applied.

One of the interesting features of our approach is that the diffusion coefficient D is not a constant. Although this does not affect the no-flux steady-state solution $\mathbf{J} = \mathbf{0}$, it does change the transient behavior of the system. In addition, this assumption allows a whole set of steady-state solutions corresponding to $\mathbf{J} = \text{const}$.

A. Linear stability theory

In this section we study the short-time behavior of a binary mixture, initially at uniform concentration $\phi = \phi_0$, which is suddenly quenched to a temperature well below its critical value T_c . Now the linear theory of spinodal decomposition is well known, and can be found elsewhere [12-15]; here we derive only the results that will be used in Sec. III B, where the nonlinear effects are discussed.

First, we linearize the equation of motion (28), defining

$$u = \frac{\phi - \phi_0}{\phi_0}, \quad \psi = \Psi_+ - 3(1-2\phi_0)\Psi_- - \frac{1}{2\phi_0(1-\phi_0)}, \quad (31)$$

with $u \ll 1$ and $\bar{u} = 0$, obtaining

$$\frac{\partial u}{\partial t} = -2\psi\nabla^2 u - \nabla^4 u, \quad (32)$$

where the spatial and time coordinates have been nondimensionalized in terms of a and $a^2/D(\phi_0)$, respectively.

Equation (32) is the linearized Kuramoto-Shivashinsky equation, and as such it exhibits the same behavior. In particular, $\psi \leq 0$ is a necessary condition to have instability, so that the stability condition becomes

$$[3\phi_0 - 1]\Psi_A + [3(1 - \phi_0) - 1]\Psi_B \leq \frac{1}{2\phi_0(1 - \phi_0)}. \quad (33)$$

The generalized free energy (18) and the energy dissipation (29) can be linearized in the same way, obtaining, upon integration by parts,

$$\frac{\Delta \bar{g}}{RT} = \frac{1}{2}\phi_0^2(-2\psi \bar{u}^2 + |\nabla u|^2), \quad (34)$$

$$\frac{\bar{E}}{RT} = \phi_0^2(4\psi^2 |\nabla u|^2 - 8\psi (\nabla^2 u)^2 + |\nabla^3 u|^2), \quad (35)$$

where we have defined $\Delta \bar{g} = \bar{g} - g(\phi_0)$. These expressions identically satisfy the energy conservation constraint (30).

Now, assuming a periodic perturbation for u ,

$$u = u_0 \cos(k_x x) \cos(k_y y) \cos(k_z z) e^{\sigma t}, \quad (36)$$

Eq. (32) gives

$$\sigma = k^2(2\psi - k^2), \quad (37)$$

where k is the length of the wave vector, i.e., $k^2 = k_x^2 + k_y^2 + k_z^2$. We therefore conclude that the state $\phi = \phi_0$ is unstable whenever

$$k < \sqrt{2\psi} = 2\pi a / \lambda_{\min}, \quad (38)$$

in agreement with the analysis of the steady periodic solutions of Eq. (21) developed in Sec. II. In addition, from expression (34), we find that the change in energy caused by perturbation (36) is negative, i.e., that the perturbation reduces the level of energy in the system:

$$\Delta \bar{g} = \frac{RT}{16} u_0^2 (-2\psi + k^2) e^{2\sigma t}. \quad (39)$$

Such perturbations are called negative energy perturbations [24], and can be sustained only when energy is re-

moved from the system, in this case by dissipation. The instability can therefore be called resistive [24].

Among the infinite number of unstable modes in the system, the one that grows fastest will eventually prevail. From Eq. (37) we find that the length of the wave vector $k = k_{\max}$ which maximizes the exponential growth σ is given by

$$k_{\max} = \sqrt{\psi}. \quad (40)$$

The spatial period of the solution, i.e., the typical dimension of a drop, λ , and the typical time scale of the dynamical process, τ , are, respectively, in dimensional form,

$$\lambda_s = \frac{2\pi a}{\sqrt{\psi}}, \quad \tau_s = \frac{2\pi a^2}{D(\phi_0)\psi}. \quad (41)$$

Considering that $\psi \propto (T_c - T)$ [8], this result shows that deeper quenches, corresponding to higher values of ψ , cause the formation of smaller drops within shorter times. However, this conclusion should be taken *cum grano salis*, as it assumes an instantaneous temperature quench, which is generally impossible to achieve in most experiments.

B. Effect of nonlinear terms

The diffusion coefficient D describes both the diffusion of species A into B and that of B into A , that is $D = D_{AB} = D_{BA}$. Therefore D is a function of $\phi(1 - \phi)$ and, in fact, in most cases we can assume that [23]

$$D(\phi) = D_0 \phi(1 - \phi). \quad (42)$$

This expression satisfies the trivial requirement that D must be zero as $\phi = 0$ and 1 and approximates the diffusion coefficient up to terms of order $[\phi(1 - \phi)]^3$. The diffusion coefficient must satisfy the additional requirement that it is negative (i.e., we have "negative diffusion") whenever ϕ is negative or larger than 1. Therefore, the next term in the expansion of D , i.e., the $O([\phi(1 - \phi)]^2)$ term, must be identically zero. Finally, substituting (42), (10), and (20) into (26) and (28), we obtain the unsteady governing equation

$$\begin{aligned} \phi_0(1 - \phi_0) \frac{\partial \phi}{\partial t} = & \{1 - 2\phi(1 - \phi)[\Psi_+ - 3(1 - 2\phi)\Psi_-]\} \nabla^2 \phi - (1 - 2\phi)(\nabla \phi) \cdot (\nabla^3 \phi) \\ & - 2[(1 - 2\phi)\Psi_+ - 3(1 - 6\phi + 6\phi^2)\Psi_-] |\nabla \phi|^2 - \phi(1 - \phi)(\nabla^4 \phi), \end{aligned} \quad (43)$$

where, as before, the spatial and time coordinates have been nondimensionalized in terms of a and $a^2/D(\phi_0)$, respectively. Clearly, this equation remains invariant if ϕ and Ψ_A are interchanged with $(1 - \phi)$ and Ψ_B , respectively. Equation (43) is subjected to no-flux boundary conditions so that it identically satisfies the constraint (17) of mass conservation. Equation (43) has not been written down explicitly before, to our knowledge, although its linear approximation has been studied in

previous works [12–15]. One of its main characteristics is that, unlike the original Cahn-Hilliard equation [8], it does reduce to the usual diffusion equation when ϕ is small and $\Psi_A = \Psi_B = 0$. Equation (43) can be greatly simplified when $\Psi_- = 0$, $\Psi_+ = \Psi$, and $\phi_0 = \frac{1}{2}$, obtaining

$$\frac{\partial u}{\partial t} = 4\nabla^2 u - \nabla[(1 - u^2)(2\Psi + \nabla^2)] \nabla u, \quad (44)$$

where $u = 2\phi - 1$. In order to investigate the effect of nonlinear terms, the governing equations (43) and (44) have been integrated in one-dimensional space using the spectral method described in Appendix B. The spatial coordinate was scaled through the length scale of maximum growth, $a/\sqrt{\psi}$, and time through $a^2/D(\phi_0)$.

It was found that nonlinearities saturate the growth of the instability and lead to a steady state with periodic variations of ϕ , whose period λ corresponds to the fastest growing mode of the linear regime. More exactly, we found that the final steady state of the system has a wavelength equal to the submultiple of the length of the

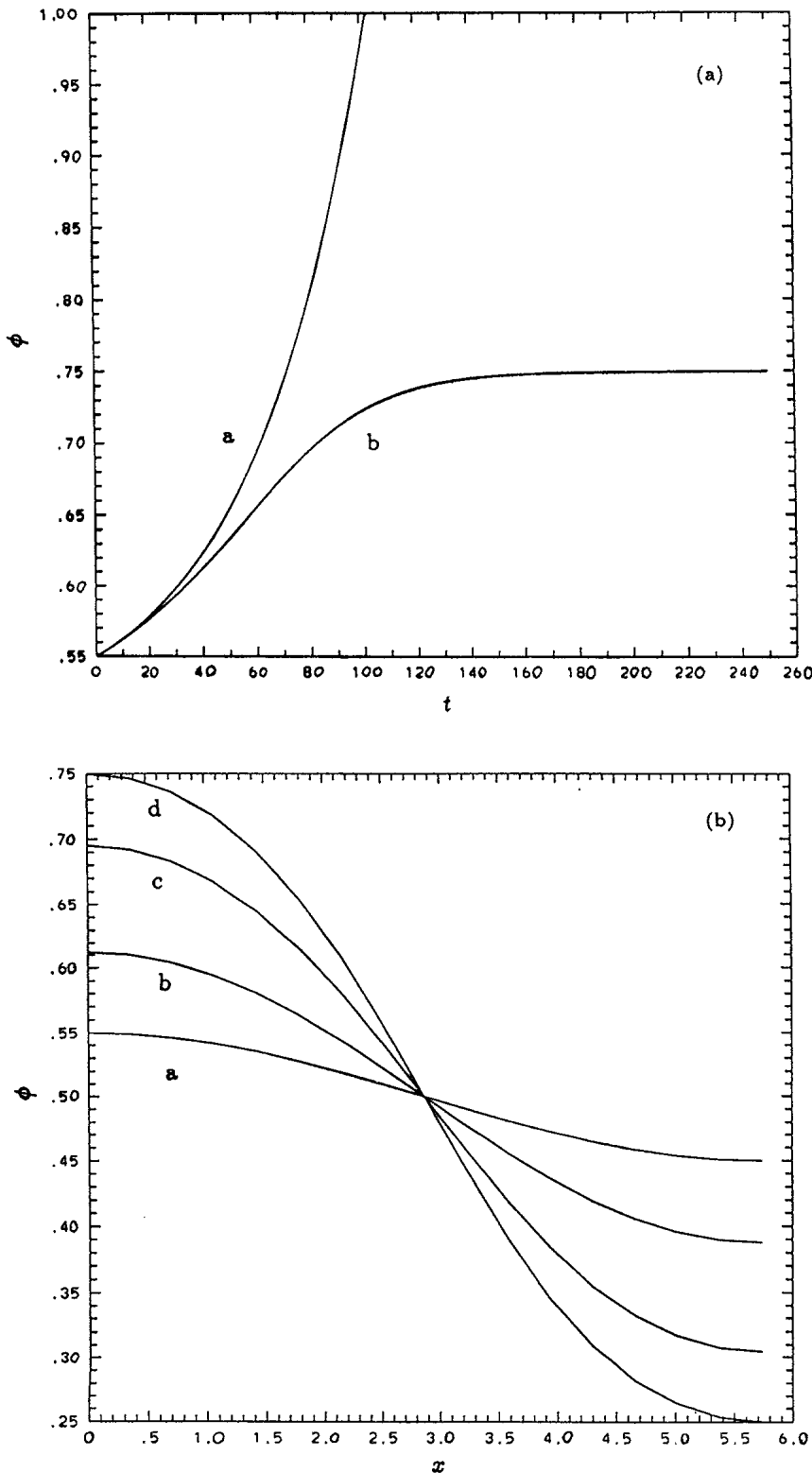


FIG. 2. (a) Composition as a function of time at a fixed location $x = 0$ for $\Psi = 2.3$. Curve *a*: linear theory, growing exponentially in time. Curve *b*: Numerical solution of Eq. (43). The numerical solution saturates gradually, reaching another equilibrium state. (b) Composition as a function of position for $\Psi = 2.3$ at different times when a small periodic perturbation with period λ_s is superimposed on the initial composition $\phi_0 = 0.5$. The spatial coordinate x is normalized to vary between 0 and π . Curves *a*, *b*, *c*, and *d* correspond, respectively, to times $t = 0, 40, 80$, and 250.

integration domain that is closest to the fastest growing mode. Therefore, since the larger the domain the closer this wavelength comes to the fastest growing mode, we have chosen the length of the domain to be an exact multiple of the fastest growing wave, out of convenience.

In Figs. 2(a) and 3(a) the composition of the mixture at

a fixed point is plotted as a function of time for two different values of Ψ , one close to the instability threshold (i.e., $\Psi = 2.3$), and the other one larger (i.e., $\Psi = 5$). Our results show that for short times an exponential growth occurs, in perfect agreement with the linear stability analysis of Sec. III A, while after a characteristic time τ_s that

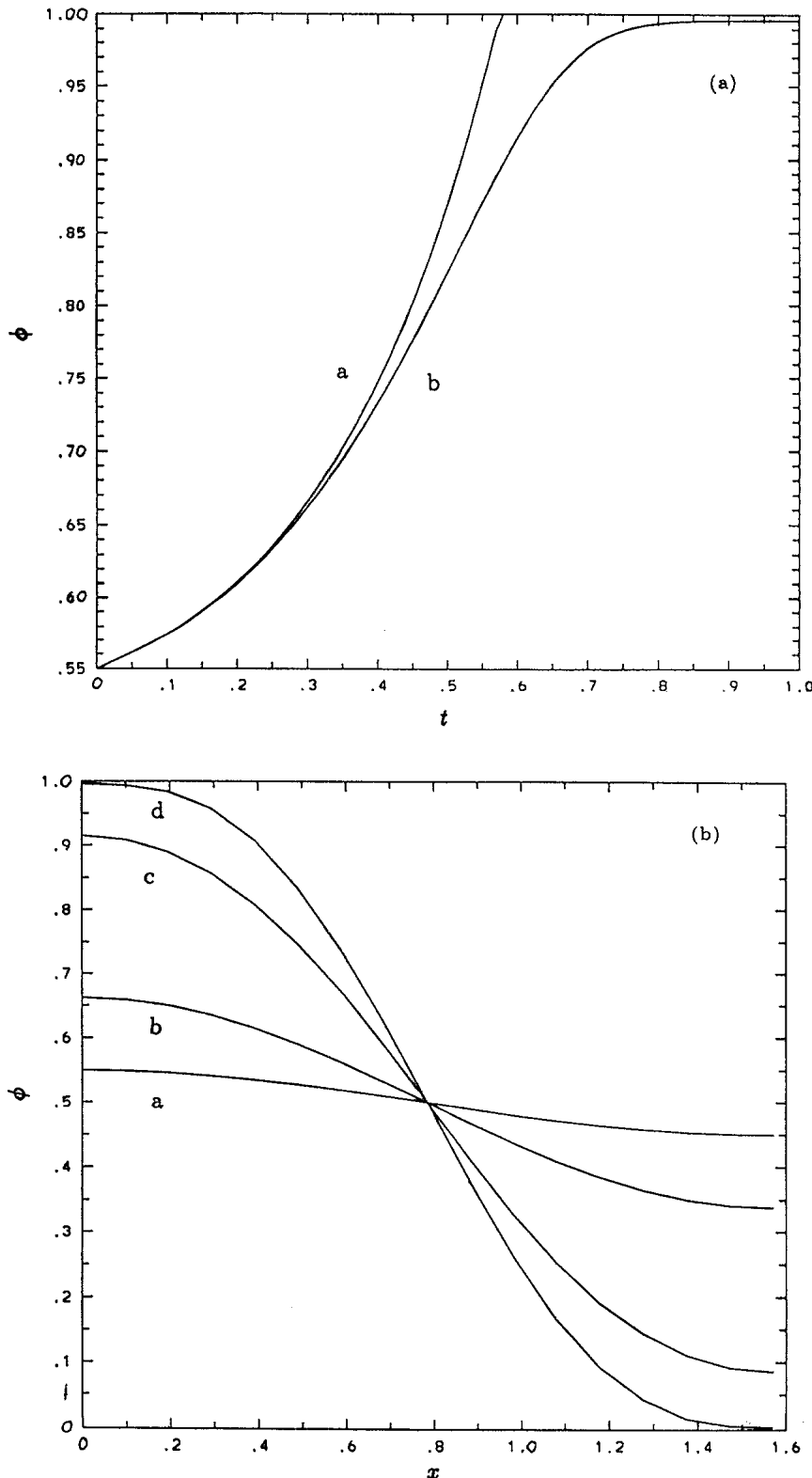


FIG. 3. (a) Composition as a function of time at a fixed location $x = 0$ for $\Psi = 5$. Curve a: Linear theory, growing exponentially in time. Curve b: Numerical solution of Eq. (43). The growth saturates much faster than in Fig. 2(a). (b) Composition as a function of position for $\Psi = 5$ at different times when a small periodic perturbation with period λ_s is superimposed on the initial composition $\phi_0 = 0.5$. The spatial coordinate x is normalized to vary between 0 and π . Curves a, b, c, and d correspond, respectively, to times $t = 0, 0.3, 0.6$, and 1.0.

agrees with Eq. (41) the solution saturates, as nonlinear effects become dominant. The complete time- and space-dependent solution of Eq. (44) can be seen in Figs. 2(b) and 3(b) for $\Psi = 2.3$ and 5, respectively. In both cases the initial composition is the same, $\phi_0 = \frac{1}{2}$, and the per-

turbation is periodic with period λ_s . As expected from the symmetry of the equation, the deviations from the initial composition remain at all times symmetric around $\phi = \frac{1}{2}$. Eventually, after a time of order τ_s , a steady-state configuration is reached that, for $\Psi = 2.3$, agrees within

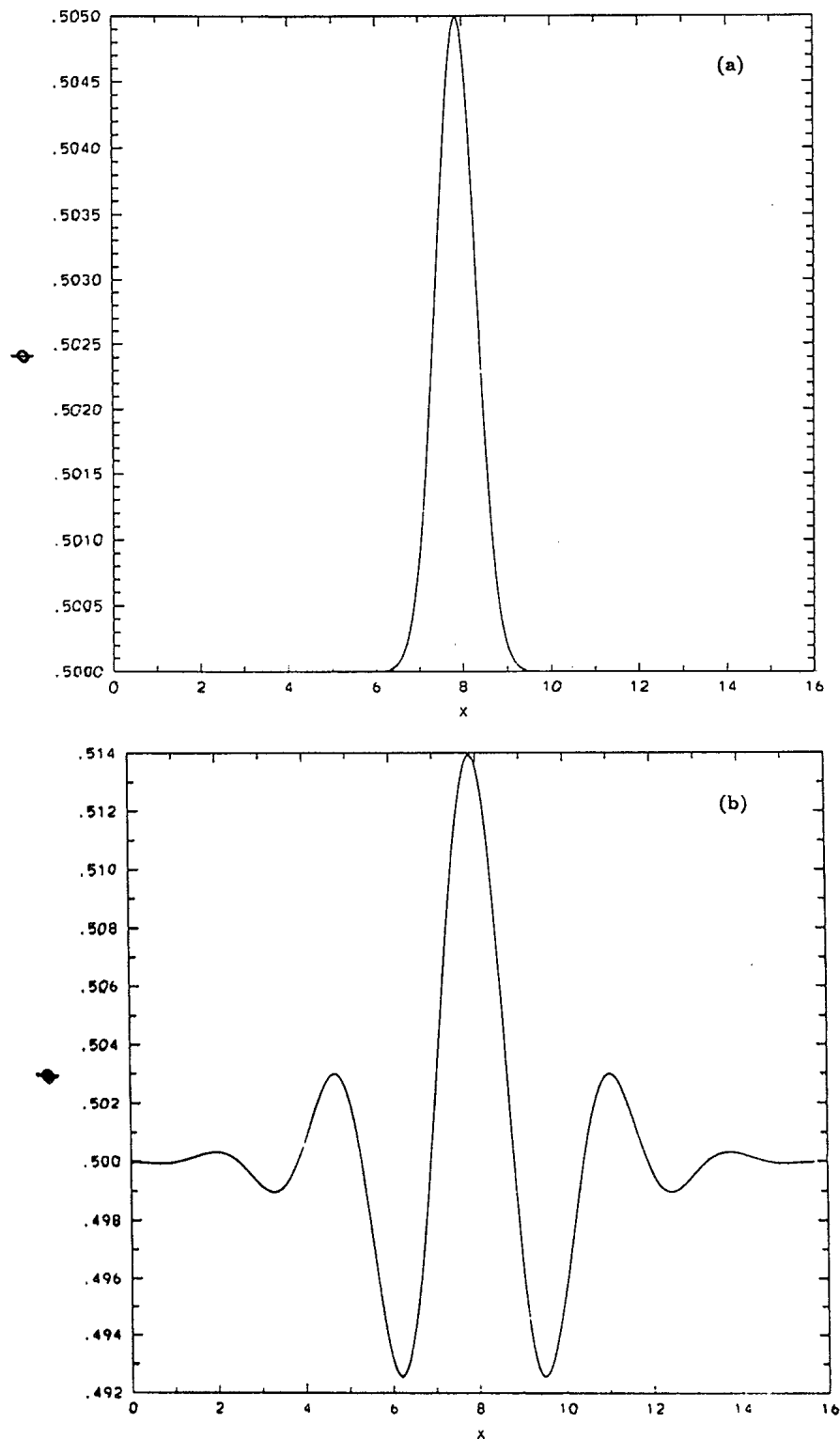


FIG. 4. Composition as a function of position for $\Psi = 5$ at different times when a small localized perturbation is superimposed to the initial composition $\phi_0 = 0.5$. The spatial coordinate x is normalized to vary between 0 and 8π . (a), (b), and (c) correspond, respectively, to times $t = 0, 0.5$, and 3.

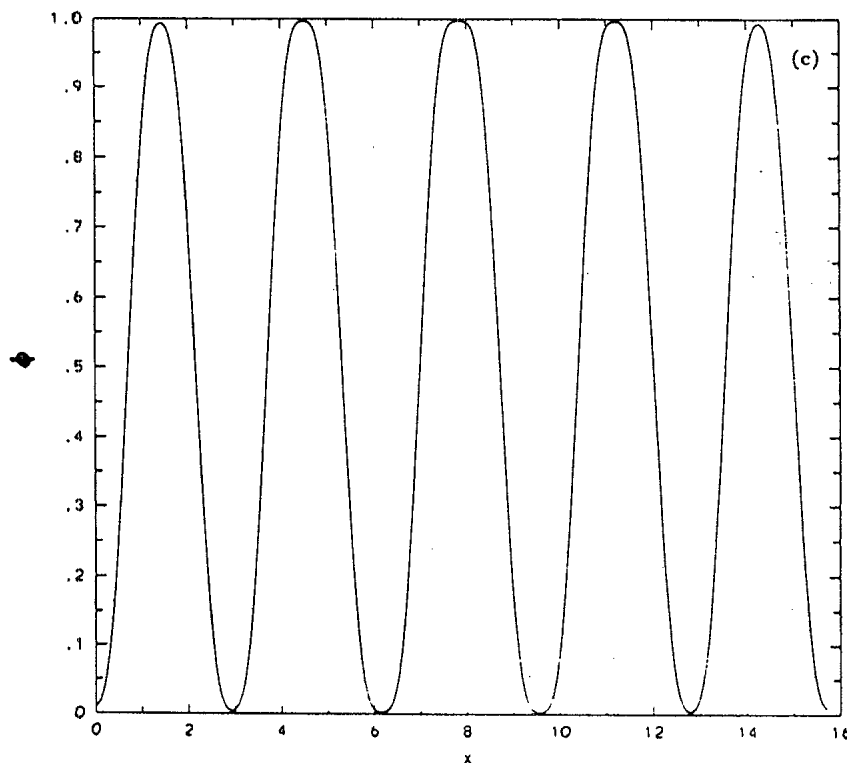


FIG. 4. (Continued).

1% with the periodic solution (23) with period λ_s . Specifically, this solution corresponds to a value $\alpha = 0.933$ of the slope of the steady concentration profile at the origin. We note here that the analytical solution (23) is only approximate, as $O(u^5)$ terms have been neglected, and in fact it is not applicable to the case $\Psi = 5$. Therefore, we see that a broadband initial excitation of the system selects the fastest growing mode. This behavior is quite typical of absolutely unstable supercritical systems, where the fastest-growing mode is also the absolute instability mode of the system, as it corresponds to the pinching double root of the dispersion relation. Finally, it should be noted that while for $\Psi = 2.3$ the Ginzburg criterion (19) is satisfied, when $\Psi = 5$ it is not, and this case is presented only to illustrate the main features of our model. However, this limitation is not too severe, as, for example, the case $\Psi = 2.3$, far from being ideal, describes the state of any binary mixture whose equilibrium compositions are $\phi_e = 0.16$ and 0.84 [see Eqs. (12) and (13)]. So, for example, this case describes the mixture nitromethane-pentene, with a critical temperature $T_c = 47^\circ\text{C}$ [25], when it is quenched to 30°C .

An important result of our computation is that the final steady-state concentration profile is independent of the initial disturbance, provided that this disturbance is small. This can be seen in Fig. 4, where the case with $\Psi = 5$ and $\phi_0 = \frac{1}{2}$ is analyzed, assuming that the initial perturbation is localized. Our results show that eventually the system reaches the same steady state as the one of Fig. 3(b). However, the relaxation time in this case depends on the dimension of the system, as one would expect, given the diffusive nature of the process. For

example, in the computation of Fig. 4 the system has a width of $8\lambda_s$, and the relaxation time is about three times larger than in the previous case, where the system effectively has a width equal to λ_s . The independence of the final stationary profile from its initial conditions was not noticed in the previous numerical solution of the Cahn-Hilliard equation [26].

Another important result of our computation is that the concentration within the drops at steady state, ϕ_{ss} , is position dependent, and has a metastable value, lying between its equilibrium and its spinodal value, i.e.,

$$|\phi_e(T) - \frac{1}{2}| > |\phi_{ss}(T) - \frac{1}{2}| > |\phi_s(T) - \frac{1}{2}|. \quad (45)$$

This behavior can be understood by noting that in the steady-state solution, Eq. (20) with $\gamma = 0$, the nonzero chemical potential term is equal to the Laplacian of the concentration, thereby implying that the steady-state concentration within a drop is not constant in space. So we conclude that, once the unstable, spinodal decomposition process is completed, a stationary configuration ϕ_{ss} is reached, corresponding to the formation of small, metastable drops. Later, these metastable drops will grow with time, due to thermal fluctuations, coalescence, and gravity, until a complete phase separation is achieved. This successive coarsening process takes place with much longer characteristic times and will be addressed in a future study.

For different values of the initial concentration ϕ_0 and when $\Psi_A \neq \Psi_B$, we obtained results that are qualitatively similar to the ones described in Figs. 2, 3, and 4, so that we chose not to include them.

ACKNOWLEDGMENT

R.M. and R.S. were supported in part by Grant No. CTS-9216133 from the National Science Foundation.

APPENDIX A: EXCESS FREE ENERGY

From the definition of the excess free energy, $g^{\text{ex}} = g - g^{\text{id}}$, and the energy conservation equation, $dg = vdP$, at constant temperature T and composition x_A , with v and P denoting molar volume and pressure, respectively, we easily find, at constant temperature and composition [23]

$$g^{\text{ex}} = RT \int_0^P (Z - 1) dP/P, \quad (\text{A1})$$

where R is the gas constant and $Z = Pv/RT$ the compressibility factor. Now Z can be expressed through the virial equation for a gas binary mixture [19],

$$Z = 1 + \frac{BP}{RT}, \quad B = x_A^2 B_{AA} + 2x_A x_B B_{AB} + x_B^2 B_{BB}, \quad (\text{A2})$$

where the virial coefficient B_{ij} characterizes the repulsive interaction between molecule i and molecule j ,

$$B_{ij}(T) = \frac{1}{2} \int (1 - e^{-U_{ij}/RT}) d\mathbf{r}, \quad (\text{A3})$$

with $U_{ij}(r)$ denoting the interaction energy between

molecules i and j . Finally, substituting (A2) into (A1) and assuming that, since species A and B have similar properties, $B_{AA} = B_{BB}$, we obtain the Flory-Hugging expression (5) with $\Psi = 2P(B_{AB} - B_{AA})/(RT)$. From here it appears that $\Psi > 0$ when the repulsive force between different molecules A and B is stronger than that between identical molecules.

APPENDIX B: NUMERICAL TECHNIQUE

The one-dimensional version of Eq. (44) was solved numerically, using a split-step method in time and a pseudospectral collocation method in space. In one dimension Eq. (44) reads

$$\frac{\partial u}{\partial t} = 4 \frac{\partial^2 u}{\partial x^2} - \frac{\partial}{\partial x} \left[(1 - u^2) \left(2\Psi + \frac{\partial^2}{\partial x^2} \right) \frac{\partial u}{\partial x} \right]. \quad (\text{B1})$$

In the first part of the split step we treat all nonlinear terms, whereas in the second part we only treat all linear terms.

Because of the symmetry of Eq. (B1) with respect to x (it does not change if x is replaced by $-x$), we can expand u in a cosine Fourier series in x . The truncated version of the series reads

$$u = \sum_{n=0}^N q_n \cos nx, \quad (\text{B2})$$

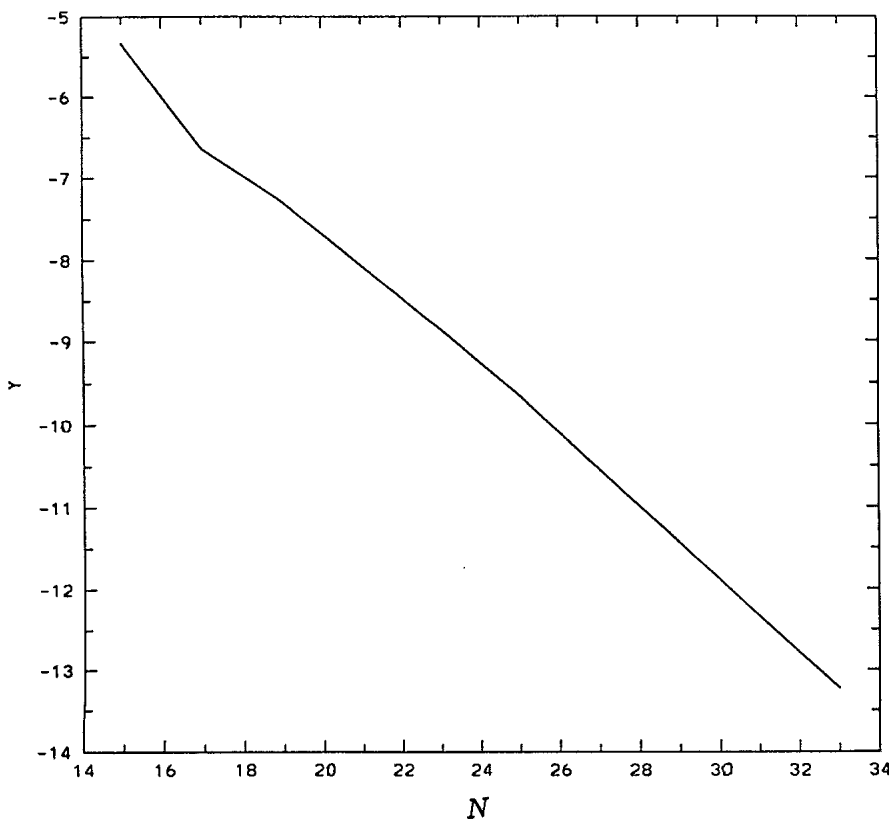


FIG. 5. Logarithm of the error in the first Fourier coefficient as a function of the number of Fourier coefficients N . The error decays exponentially with N .

where we have assumed that x varies in the interval $(0, \pi)$ (if not, a simple rescaling of x will do). Within the context of collocation methods the coefficients q_n are related to the values of u at the equidistant points $x_l = l\pi/N$, $n = 0, 1, \dots, N$ through the discrete cosine transform (see, for example, Press *et al.* [27]):

$$q_n = \sum_{l=0}^{N-1} u_l \cos\left(\frac{nl\pi}{N}\right), \quad (B3)$$

$$u_l = \frac{2}{N} \sum_{n=0}^{N-1} q_n \cos\left(\frac{nl\pi}{N}\right), \quad (B4)$$

where $u(x_l) = u_l$.

All even-order derivatives of u have cosine transforms like (B3), whereas all odd-order derivatives of u have sine transforms. The cosine and sine transforms and their inverses can be computed very efficiently using the fast Fourier transform algorithm. Thus the discrete Fourier

cosine transform of u is first evaluated, then the derivatives of u at the points $x = x_l$ are evaluated first in wave number space, and are transformed back into physical space through inverse fast Fourier transforms. The integration in time is then performed in physical space using the explicit second-order accurate Adams-Bashforth scheme [27].

In the second part of the scheme only the linear terms are treated. The integration in time is performed analytically in wave number space using the outcome of the first part of the split as an initial condition. Then the results are transformed back into physical space to proceed with the next time step.

The accuracy of the computation is first order in time because of the split. Thus the error is kept low by reducing the size of the time step. The convergence in space, on the other hand, is exponentially fast in N . This is demonstrated in Fig. 5, where the error in the first Fourier coefficient is plotted as a function of N in a semilog plot (computation for $\Psi = 3$).

- [1] P.G. deGennes, *Scaling Concepts in Polymer Physics* (Cornell University, Ithaca, NY, 1979), and reference therein.
- [2] Recent reviews of the kinetics of unmixing can be found in J.D. Gunton, M. San Miguel, and P.S. Sahni, in *Phase Transition and Critical Phenomena*, edited by C. Domb and J.L. Lebowitz (Academic, London, 1983), Vol. 8, p. 267; K. Binder, in *Condensed Matter Research Using Neutrons*, edited by S.W. Lovesey and R. Scherm (Plenum, New York, 1984), p. 1. Critical dynamics of mixtures is also reviewed in K. Kawasaki, in *Phase Transition and Critical Phenomena*, edited by C. Domb and J.L. Lebowitz (Academic, London, 1976), Vol. 5A; P.C. Hohenberg and B.I. Halperin, *Rev. Mod. Phys.* **49**, 435 (1977).
- [3] J.S. Huang, W.I. Goldberg, and Bjerkaas, *Phys. Rev. Lett.* **32**, 921 (1974); Y.C. Chou and W.I. Goldberg, *Phys. Rev. A* **20**, 2105 (1979); **23**, 858 (1981).
- [4] N.C. Wong and C.M. Knobler, *J. Chem. Phys.* **69**, 725 (1978); *Phys. Rev. A* **24**, 3205 (1981); *J. Chem. Phys.* **85**, 1972 (1981).
- [5] J.M. Lifshitz and V.V. Slyozov, *J. Phys. Chem. Solids* **19**, 35 (1961).
- [6] E.D. Siggia, *Phys. Rev. A* **20**, 595 (1979).
- [7] P. Guenoun, R. Gastaud, F. Perrot, and D. Beysens, *Phys. Rev. A* **36**, 4876 (1987); P. Guenoun, D. Beysens, and M. Robert, *Phys. Rev. Lett.* **65**, 2406 (1990); C.K. Chan, F. Perrot, and D. Beysens, *Phys. Rev. A* **43**, 1826 (1991); A. Cumming, P. Wiltzius, F.S. Bates, and J.H. Rosedale, *Phys. Rev. A* **45**, 885 (1992); D. Katsen and S. Reich, *EuroPhys. Lett.* **21**, 55 (1993); D. Beysens, P. Guenoun, and P. Sibille, *Phys. Rev. A* **50**, 1299 (1994).
- [8] J.W. Cahn and J.E. Hilliard, *J. Chem. Phys.* **28**, 258 (1958); **31**, 688 (1959).
- [9] J.S. Langer, M. Bar-on, and H.D. Miller, *Phys. Rev. A* **11**, 1417 (1975); J.S. Langer, in *Systems Far from Equilibrium*, edited by L. Garrido, Lecture Notes on Physics No. 132 (Springer-Verlag, Berlin, 1980).
- [10] K. Binder and D. Stauffer, *Phys. Rev. Lett.* **33**, 1006 (1974); K. Binder, C. Billitet, and P. Miold, *Z. Phys. B* **30**, 183 (1978); K. Binder, in *Systems Far from Equilibrium*, edited by L. Garrido, Lecture Notes on Physics No. 132 (Springer-Verlag, Berlin, 1980).
- [11] Kawasaki, *Prog. Theor. Phys.* **57**, 826 (1977); K. Kawasaki and T. Ohta, *Prog. Theor. Phys.* **59**, 362, 1406 (1978).
- [12] H.E. Cook, *Acta Metall.* **18**, 297 (1970).
- [13] P.G. deGennes, *J. Chem. Phys.* **72**, 4756 (1980).
- [14] P. Pincus, *J. Chem. Phys.* **75**, 1996 (1981).
- [15] K. Binder, *J. Chem. Phys.* **79**, 6387 (1983).
- [16] K. Binder, H.L. Frisch, and J. Jackle, *J. Chem. Phys.* **85**, 1505 (1986); K. Binder, *Phys. Rev. A* **29**, 341 (1984).
- [17] J.M. Smith and H.C. Van Ness, *Introduction to Chemical Engineering Thermodynamics* (McGraw-Hill, New York, 1987), Chap. 11.
- [18] P. Flory, *Principles of Polymer Chemistry* (Cornell University Press, Ithaca, NY, 1971), Chap. 12; M. Huggins, *J. Am. Chem. Soc.* **64**, 1712 (1942).
- [19] L.D. Landau, E.M. Lifshitz, and L.P. Pitaevskii, *Statistical Physics* (3rd ed), Pt. 1 (Pergamon, Oxford, 1978).
- [20] J.D. van der Waals, *Z. Phys. Chem.* **13**, 657 (1894), reprinted in *J. Stat. Phys.* **20**, 200 (1979); A.J.M. Yang, P.D. Fleming, and J.H. Gibbs, *J. Chem. Phys.* **64**, 3732 (1976); B.S. Carey, L.E. Scriven, and H.T. Davis, *J. Chem. Phys.* **69**, 5040 (1978); R. Evans, *Adv. Phys.* **28**, 143 (1979).
- [21] J.S. Langer, *Ann. Phys.* **65**, 53 (1971).
- [22] A. Novick Cohen and L.A. Segel, *Physica D* **10**, 277 (1984).
- [23] S.R. DeGroot and P. Mazur, *Non-Equilibrium Thermodynamics* (Dover, New York, 1962).
- [24] A. Bers, in *Plasma Physics, Les Houches 1972*, edited by G. DeWitt and J. Peyraud (Gordon and Breach, New York, 1975).
- [25] E.A. Macedo and P. Rasmussen, *Liquid-Liquid Equilibrium Data Collection. Supplement 1* (DECHEMA, Frankfurt, 1987).
- [26] A.B. Bortz, *J. Stat. Phys.* **11**, 181 (1974).
- [27] W.H. Press, B.R. Flannery, S.A. Teukolsky, and W.T. Vetterling, *Numerical Recipes* (Cambridge University Press, Cambridge, 1989).